TERNARY CASSON HYBRID NANOFLUIDS IN CONVERGENT/DIVERGENT CHANNEL FOR THE APPLICATION OF MEDICATION

by

Abeer S. ALNAHDI[a*], Saleem NASIR[b], and Taza GUL[c]

[a] Department of Mathematics and Statistics, Faculty of Science,
Imam Mohammad Ibn Saud Islamic University (IMSIU), Riyadh, Saudi Arabia
[b] Department of Mathematics, Faculty of Applied Science,
King Mongkut's University of Technology North Bangkok, Bangkok, Thailand
[c] Department of Mathematics, City University of Science and Information Technology,
Peshawar, Pakistan

Original scientific paper
https://doi.org/10.2298/TSCI23S1067A

The mathematical analysis of time-independent mobility of a modified blood-based Casson hybrid nanofluid including dissimilar nanomaterials in a convergent/divergent channel with stretchable/shrinkable walls is investigated. The cumulative impact of magnetic and electric fields governs the flow of modified hybrid nanofluids. In this study, a mediated hybrid fluid containing three unique nanomaterials (titania oxide, alumina oxide, and silver nanoparticles) is used to evaluate the efficiency of hybrid nanofluids in collaboration with blood as a base fluid. The flow analysis is performed using long-wavelength estimations and creeping processes. Such computational innovation will also be used to investigate the transmission of biofluids from big to smaller arteries and intestines. The homotopy analysis method is used to generate the analytical solutions for a system of non-dimensional boundary value problems. Utilizing MATHEMATICA software, the impacts of model physical parameters on rheological phenomena are visually illustrated. The mathematical model can be used to transmit complex biofluids and control fluid transit by employing electro-kinetic modification technologies. To verify the current findings, a comparable investigation is developed.

Key words: *electromagnetic filed, stretchable/shrinkable walls, Casson fluid, tri-hybrid nanofluid, drug delivery, heat absorption/omission, HAM*

Introduction

In literature biomedical nanostructures have recently received a lot of attention due to its wide range biomedical uses and biological properties. The considerable advancement of nanoparticles especially nanocomposites in the biomedicine area has potential and far-reaching implications, particularly for anticancer gene/drug transport, antimicrobial, biosensors, biomedical imaging, enzymes, drug carriers, nucleic acids, vaccinations and genetics [1-3]. These nanomaterials are biocompatible and have electromagnetic, pharmacological, structural and thermal properties. Furthermore, the Ag, TiO_2, and Al_2O_3 nanocomposites are harmless in biological materials. Silver nanomaterials have a distinct photonic behavior that is important for a variety of remedial uses like photodynamic therapy and radio waves for cancer cell eradication and diag-

* Corresponding author, e-mail: asalnahdi@imamu.edu.sa

nosing purposes like cell imagination, computed imaging and ophthalmic tomography. Fullstone *et al.* [4] developed a nanoparticles operative simulation for the circulation of blood through vessels. The magnetic nanoparticles-based concept for the progress of more sophisticated medicinal uses was presented by Li *et al.* [5]. Ijaz and Nadeem [6] and Dykmana and Khlebtsov [7] have disclosed some important works on nanofluid-flow with drug assessments in various configuration. Various scientists [8, 9] have addressed a thermophysical feature of hybrid nanofluid in experimental analysis, which is leading to advancements in heat production of liquids. To optimize the characteristics of materials, hybrid nanofluid is comprised of two or more nanometer-sized particles. Industrial, marine constructions, transport, acoustics, defensive performance, micro-fluidics, pharmaceutical and other engineering disciplines use hybrid nanofluids for heat transmission [10]. To better understand the rheological and heat exchange features of hybrid nanofluid-flow and heat transfer assessment, conceptual and numerical simulations have been conducted in recent years. Waqas *et al.* [11] numerically examined the energy transmission of aluminum alloy blood-based hybrid nanofluid in rotating channel along with energy source and non-linear radiation. Hussain *et al*. [12], Ramzan *et al*. [13], and Hassan *et al.* [14] are a few additional notable works explaining the hybrid nanofluid energy transmission mechanism and its applications in various sectors of science and technology.

Biomagnetic liquids are physiologic liquids that are influenced by applied magnetic field and magnetism. Recently biomagnetic liquid has received a lot of attention because it has a variety of applications in biomedical and bioengineering, such as medication delivery systems, cell imaging, magnetize looped treatment, reduced bleeding during surgical operations, magnetic hyperthermia, medical instruments like magnetic detectors and plasma compressors. Therefore, it is perceived that blood is one of the pertinent forms of biomagnetic fluid because it contains the cellular membranes, the composite interface of hemoglobin and extracellular protein. Furthermore, purified blood is less affected by the magnetism. It has been revealed that artificially sustaining nanomaterials having magnetic properties can significantly increase blood magnetism. Also, blood carrying those nanocomposites denies magnetization or discards diamagnetic material, causing it to behave as a ferromagnetic fluid, with a steady increase in fluid velocity. Mousavi *et al.* [15] studied the dynamics of biomagnetic liquid over a regular tube along with magnetic dipole and Lorentz force and they determined that the frictional force in the restricted region reduces the yield stress. The works of Bhatti *et al*. [16], Abdelsalam *et al.* [17], Bhaumik *et al.* [18], and Mekheimer *et al*. [19] highlight some significant investigations on blood flow with the impact of the magnetic field.

Because of its many industrial, technical and manufacturing applications, the flow characteristics across a converging/diverging channels is becoming incredibly valuable. Enhancement of energy transmission rate in thermal storage technique for milk flow, melted polymeric extruded using convergent die, cooler drafting process in production of polymers*, etc.* [20]. Pumping of blood via arteries and capillaries in the human body is another evidence of liquid dynamics through converging/diverging channels. In the beginning, Jeffery [21] and Hamel [22] lay-out the groundwork for flow via converging/diverging channels. Numerous scholars have produced extremely effective investigations on the Jeffery-Hamel flow in the presence of temperature distribution following their groundbreaking work. Dogonchi and Ganji [23] investigated the dynamics of nanofluid among two non-parallel boundaries using Brownian diffusion and thermophoresis. Zheng *et al.* [24] has performed a computational study that looked at heat transport across convergent/divergent slit ribs. Ahmed *et al.* [25] and Mishra *et al.* [26] investigated the same flow model employing the idea of shrinking/extending in converging and diverging channels.

In light of this comprehensive existing literature, it is noteworthy that further research into the coupled effect of electromagnetic and Ohmic heating on energy transport and flow of Casson (TiO_2-Al_2O_3-Ag/blood) tri-hybrid nanofluid about a shrinking/stretching in converging/diverging channels has never been investigated before. The following aspects of the current investigation are distinctive:

– The flow of blood based tri-hybrid nanofluid through stretching/shrinking in converging and diverging channel.
– Impact of (TiO_2-Al_2O_3-Ag/blood) tri-hybrid nanofluid on energy distributions and flow structures.
– Examine the dynamics of suitable background of Casson tri-hybrid nanofluid.
– The mechanism of electromagnetic, Ohmic heating and viscous dissipations further strengthen the novelty of analysis.

The non-similar reduction is applied to the modelled governing equations and associated boundary constraints. Furthermore, using the HAM technique, the resultant equations are evaluated for solution transformations.

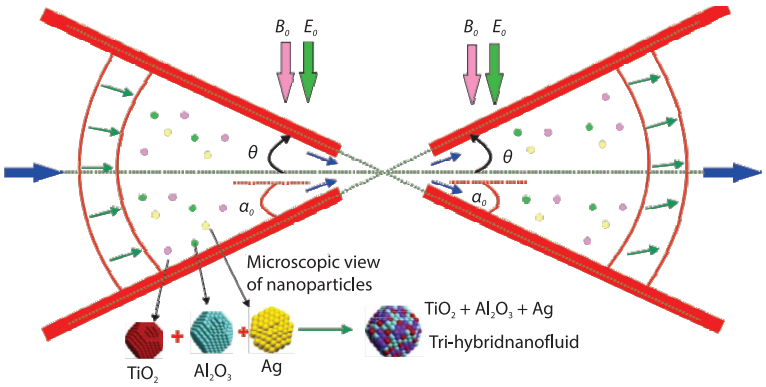

Figure 1. Schematic geometry of the flow

Formulation

Consider time independent, 2-D, incompressible Casson flow of electromagnetic tri-hybrid nanofluid via convergent-divergent channel link between two shrinkable and expandable non-intersecting plates at an inclination 2α. Figure 1 depicts a schematic representation of the current physical model. The dynamic investigation through the channel is described using cylindrical polar co-ordinates (r, θ, z). The non-intersecting walls are assumed to be divergent if $\alpha > 0$ and elsewhere convergent. The flow regime can thus be described as $V = [u(r, \theta), 0, 0]$, and the channel sides are both radially shrinkable and extensible with speed $u = sr^{-1} = u_w$. Because of the minimal magnetic Reynolds number, the magnetic and electric fields $B(r) = B_0 r^{-1}$ and $E(r) = E_0 r^{-1}$ are imposed perpendicular to the radial direction, while the induced magnetic field is ignored. The energy transmission properties are examined extensively using a tri-hybrid nanofluid comprised of three different types of nanoparticles: titania oxide, alumina oxide, and silver. The Jeffery-Hamel [21, 22] flow problem is the name given to this pattern of flow in literature. Under the hypotheses specified earlier, the mathematical description for model equations [6, 23, 26]:

$$\rho_{\text{thnf}} \left(\frac{u}{r} + \frac{\partial u}{\partial r} \right) = 0 \tag{1}$$

$$u\frac{\partial u}{\partial r}=-\frac{1}{\rho_{\text{thnf}}}\left(\frac{\partial p}{\partial r}\right)+\frac{\sigma_{\text{thnf}}}{\rho_{\text{thnf}}}\left(\frac{E_0B_0-B_0^{\,2}}{r^2}\right)u+\frac{\mu_{\text{thnf}}}{\rho_{\text{thnf}}}\left(1+\frac{1}{\beta}\right)\left(\frac{\partial^2 u}{\partial r^2}+\frac{1}{r}\frac{\partial u}{\partial r}+\frac{1}{r^2}\frac{\partial^2 u}{\partial\theta^2}-\frac{u}{r^2}\right) \tag{2}$$

$$r^2\frac{\partial p}{\partial\theta}-2\mu_{\text{thnf}}\frac{\partial u}{\partial\theta}=0 \tag{3}$$

$$\begin{aligned}\left(\rho C_p\right)_{\text{thnf}}\left(u\frac{\partial T}{\partial r}\right)&=k_{\text{thnf}}\left(\frac{\partial^2 T}{\partial r^2}+\frac{1}{r^2}\frac{\partial^2 T}{\partial\theta^2}+\frac{1}{r}\frac{\partial T}{\partial r}\right)+\frac{\sigma_{\text{thnf}}}{r^2}\left(B_0u-E_0\right)^2+\\&+\mu_{\text{thnf}}\left(1+\frac{1}{\beta}\right)\left[\frac{2u^2}{r^2}+2\left(\frac{\partial u}{\partial r}\right)^2+\frac{1}{r^2}\left(\frac{\partial u}{\partial\theta}\right)^2\right]\end{aligned} \tag{4}$$

where p, E_0, B_0, β are signified the pressure term, electric and magnetic field, and Casson fluid factor. Here ρ_{hnf}, σ_{hnf}, k_{hnf}, and $(\rho C_p)_{\text{hnf}}$ are the density, electrical and thermal conductivities, and specific heat of tri-hybrid nanofluid which is defined in eqs. (5)-(9). Table 1 also provides the numerical values of thermophysical characteristics of nanoparticles and the base fluid:

$$\frac{\mu_{\text{thnf}}}{\mu_{\text{f}}}=\frac{1}{(1-\phi_{\text{TiO}_2})^{2.5}(1-\phi_{\text{Ag}})^{2.5}(1-\phi_{\text{Al}_2\text{O}_3})^{2.5}} \tag{5}$$

$$\frac{\rho_{\text{thnf}}}{\rho_{\text{f}}}=\left(1-\phi_{\text{TiO}_2}\right)\left[\left(1-\phi_{\text{Ag}}\right)\left\{\left(1-\phi_{\text{Al}_2\text{O}_3}\right)+\phi_{\text{Al}_2\text{O}_3}\frac{\rho_{\text{Al}_2\text{O}_3}}{\rho_{\text{f}}}\right\}+\phi_{\text{Ag}}\frac{\rho_{\text{Ag}}}{\rho_{\text{f}}}\right]+\phi_{\text{TiO}_2}\frac{\rho_{\text{TiO}_2}}{\rho_{\text{f}}} \tag{6}$$

$$\begin{aligned}&\frac{k_{\text{thnf}}}{k_{\text{hnf}}}=\left[\frac{k_{\text{TiO}_2}+2k_{\text{hnf}}-2\phi_{\text{TiO}_2}\left(k_{\text{hnf}}-k_{\text{TiO}_2}\right)}{k_{\text{TiO}_2}+2k_{\text{hnf}}+\phi_{\text{TiO}_2}\left(k_{\text{hnf}}-k_{\text{TiO}_2}\right)}\right],\ \frac{k_{\text{hnf}}}{k_{\text{nf}}}=\left[\frac{k_{\text{Ag}}+2k_{\text{nf}}-2\phi_{\text{Ag}}\left(k_{\text{nf}}-k_{\text{Ag}}\right)}{k_{\text{Ag}}+2k_{\text{nf}}+\phi_{\text{Ag}}\left(k_{\text{nf}}-k_{\text{Ag}}\right)}\right]\\&\frac{k_{\text{nf}}}{k_{\text{f}}}=\left[\frac{k_{\text{Al}_2\text{O}_3}+2k_f-2\phi_{\text{Al}_2\text{O}_3}\left(k_{\text{f}}-k_{\text{Al}_2\text{O}_3}\right)}{k_{Al_2O_3}+2k_{\text{f}}+\phi_{\text{Al}_2\text{O}_3}\left(k_{\text{f}}-k_{\text{Al}_2\text{O}_3}\right)}\right]\end{aligned} \tag{7}$$

$$\begin{aligned}\frac{(\rho Cp)_{\text{thnf}}}{\left(\rho C_p\right)_{\text{f}}}&=\left(1-\phi_{\text{TiO}_2}\right)\left[\left(1-\phi_{\text{Ag}}\right)\left\{\left(1-\phi_{\text{Al}_2\text{O}_3}\right)+\phi_{\text{Al}_2\text{O}_3}\frac{\left(\rho C_p\right)_{\text{Al}_2\text{O}_3}}{\left(\rho C_p\right)_f}\right\}+\phi_{\text{Ag}}\frac{\left(\rho C_p\right)_{\text{Ag}}}{\left(\rho C_p\right)_f}\right]+\\&+\phi_{\text{TiO}_2}\frac{\left(\rho Cp\right)_{\text{TiO}_2}}{\left(\rho Cp\right)_f}\end{aligned} \tag{8}$$

$$\begin{aligned}&\frac{\sigma_{\text{thnf}}}{\sigma_{\text{hnf}}}=\frac{\left(1+2\phi_{\text{TiO}_2}\right)\sigma_{\text{TiO}_2}+\left(1-2\phi_{\text{TiO}_2}\right)\sigma_{\text{hnf}}}{\left(1-\phi_{\text{TiO}_2}\right)\sigma_{\text{TiO}_2}+\left(1+\phi_{\text{TiO}_2}\right)\sigma_{\text{hnf}}},\ \frac{\sigma_{\text{hnf}}}{\sigma_{\text{nf}}}=\frac{\left(1+2\phi_{\text{Ag}}\right)\sigma_{\text{Ag}}+\left(1-2\phi_{\text{Ag}}\right)\sigma_{\text{nf}}}{\left(1-\phi_{\text{Ag}}\right)\sigma_{\text{Ag}}+\left(1+\phi_{\text{Ag}}\right)\sigma_{\text{nf}}}\\&\frac{\sigma_{\text{nf}}}{\sigma_{\text{f}}}=\frac{\left(1+2\phi_{\text{Al}_2\text{O}_3}\right)\sigma_{\text{Al}_2\text{O}_3}+\left(1-2\phi_{\text{Al}_2\text{O}_3}\right)\sigma_{\text{f}}}{\left(1-\phi_{Al_2O_3}\right)\sigma_{\text{Al}_2\text{O}_3}+\left(1+\phi_{\text{Al}_2\text{O}_3}\right)\sigma_{\text{f}}}\end{aligned} \tag{9}$$

Table 1. The numerical thermophysical characteristics of nanomaterials and base fluids [6]

Nanomaterial	c_p [Jkg^{-1}K^{-1}]	k [Wm^{-1}K^{-1}]	ρ [kgm^{-3}]
TiO_2	686.2	8.954	4250
Al_2O_3	765	40	3970
Ag	235	429	10500
Blood	3594	0.492	1063

The following are the appropriate boundary constraints for the proposed physical equation [26]:

$$\begin{gathered}\text{At } \theta \to 0, r \neq 0,\ u = u_c r^{-1},\ \frac{\partial T}{\partial \theta} = u\left(\frac{\partial T}{\partial r}\right) = 0 \\ \text{as } \theta \to \pm\alpha,\ u = sr^{-1} = u_w,\ T = T_w r^{-2}\end{gathered} \tag{10}$$

For the radial flow situation eq. (1) can be described:

$$r^{-1} f(\theta) = u(r, \theta) \tag{11}$$

To make the governing eqs. (2)-(4) simpler, we firstly omit the pressure factor from eqs. (2) and (3). The similarity transformations will be implemented after that:

$$f(\eta) = \left(u_c\right)^{-1} f(\theta),\ \Theta(\eta) = \left(r^2 T\right) T_w^{-1},\ \eta = \theta\alpha^{-1} \tag{12}$$

In light of eqs. (5) and (9) and tab. 1, we have from eqs. (2)-(4) as:

$$\frac{\mu_{\text{thnf}}}{\mu_f}\frac{\rho_f}{\rho_{\text{thnf}}}\left(1+\frac{1}{\beta}\right) f''' - 2\alpha \,\text{Re}\, ff' - \frac{\rho_f}{\rho_{\text{thnf}}}\left[\alpha^2\left(E - f'\right) - 4\right] = 0 \tag{13}$$

$$\begin{gathered}\frac{k_{\text{thnf}}}{k_f}\text{Re}\,\Theta'' + \alpha^2 \text{Re}\left[4 + \frac{\left(\rho C_p\right)_{\text{thnf}}}{\left(\rho C_p\right)_f} 2\,\text{Pr}\, f\Theta\right] + \\ +\alpha\frac{\sigma_{\text{thnf}}}{\sigma_f} M\,\text{Re}\,\text{Pr}\,\text{Ec}\left(f - E\right)^2 + \frac{\mu_{\text{thnf}}}{\mu_f}\text{Pr}\,\text{Ec}\left[4\alpha^2 f^2 + \left(f'\right)^2\right] = 0\end{gathered} \tag{14}$$

The transformed boundary conditions in the shape of $f(\eta)$ and $\theta(\eta)$:

$$\Theta'(0) = 0 = f'(0),\quad f(0) = 1,\quad f(\pm 1) = \lambda,\quad \Theta(\pm 1) = 1 \tag{15}$$

where $\lambda = \dfrac{s}{u_c} < 0$ and $\lambda = \dfrac{s}{u_c} > 0$ are shrinking and stretching factors,

$\text{Pr} = \dfrac{\left(\mu C_p\right)_f}{k_f}$ *is* Prandtl number, $M = \dfrac{r\sigma_f B_0^2}{u_c \rho_f}$ are magnetic and electric fields,

$\text{Re} = \dfrac{r\alpha u_c}{\nu_f}$ *the* Reynolds numver, and $\text{Ec} = \dfrac{u_c^2}{T_w\left(C_p\right)_f}$ is Eckert number.

Discussion of results

The significant effects of several emergent flow factors M, α, E, and ϕ_{TiO_2}, ϕ_{Ag}, $\phi_{Al_2O_3}$ on blood flow along with nanomaterials are depicted using tabular and visualizationols of

$f(\eta)$ and $\Theta(\eta)$ Nusselt number, and C_f. For blood, we use Pr = 21 and a human body temperature of 310 K [6, 27]. The default settings for numerical computation are Ec = 0.1, Re = –25, $\beta = 0.5$ during this whole exploration. Any deviation from the default is noted in the appropriate tables and figures. In addition, the experimental data of the investigated base fluid and nanoparticles are employed in the pictorial set-ups shown in tabs. 1 and 2.

Table 2. Comparative analysis amongst the present and published work

Re	$f''(\pm1)$ ($\alpha = 5°$) [23]	$f''(\pm1)$ ($\alpha = 5°$) [25]	$f''(\pm1)$ ($\alpha = 5°$) [26]	$f''(\pm1)$ ($\alpha = 5°$) [Present]	$f''(\pm1)$ ($\alpha = –5°$) [23]	$f''(\pm1)$ ($\alpha = –5°$) [25]	$f''(\pm1)$ ($\alpha = –5°$) [26]	$f''(\pm1)$ ($\alpha = –5°$) [Present]
3	1.9883	1.9884	1.9885	1.98857	0.8524	0.8525	0.8526	0.85264
4	2.1067	2.1068	2.1069	2.10693	0.9245	0.9246	0.9247	0.92473
5	2.2142	2.2144	2.2145	2.21454	0.9621	0.9622	0.9623	0.96235

Table 3. Relationship of certain factors with –ReCf

ϕ_{TiO_2} ϕ_{Ag} $\phi_{Al_2O_3}$	M	E	β	$-ReC_f$ ($\alpha < 0$) tri-hybrid nanofluid	$-ReC_f$ ($\alpha < 0$) tri-hybrid nanofluid	$-ReC_f$ ($\alpha < 0$) tri-hybrid nanofluid	$-ReC_f$ ($\alpha > 0$) tri-hybrid nanofluid	$-ReC_f$ ($\alpha > 0$) tri-hybrid nanofluid	$-ReC_f$ ($\alpha > 0$) tri-hybrid nanofluid
0.0	0.2	0.2	0.2	0.87463	0.8574	0.8574	1.9642	1.9642	1.9642
0.02				0.8585	0.8583	0.8581	1.9664	1.9663	1.9652
0.04				0.8596	0.8592	0.8591	1.9686	1.9685	1.9673
	0.4			0.8588	0.8586	0.8585	1.9654	1.9653	1.9642
	0.6			0.8601	0.8600	0.8594	1.9665	1.9664	1.9653
		0.4		0.8542	0.8540	0.8538	1.9631	1.9630	1.9624
		0.6		0.8521	0.8520	0.8511	1.9624	1.9623	1.9618
			0.4	0.8566	0.8564	0.8554	1.9655	1.9654	1.9645
			0.6	0.8587	0.8585	0.8576	1.9668	1.9667	1.9657

Table 4. Relationship of certain factors with Nux

ϕ_{TiO_2} ϕ_{Ag} $\phi_{Al_2O_3}$	M	Ec	β	–Nu ($\alpha < 0$) tri-hybrid nanofluid	–Nu ($\alpha < 0$) tri-hybrid nanofluid	–Nu ($\alpha < 0$) tri-hybrid nanofluid	–Nu ($\alpha > 0$) tri-hybrid nanofluid	–Nu ($\alpha > 0$) tri-hybrid nanofluid	–Nu ($\alpha > 0$) tri-hybrid nanofluid
0.0	0.2	0.2	0.2	10.8574	10.8574	10.8574	8.3521	8.3521	8.3521
0.02				10.8743	10.8685	10.8674	8.3722	8.3621	8.3610
0.04				10.8967	10.796	10.775	8.3787	8.3675	8.3654
	0.4			10.8676	10.8598	10.8587	8.3621	8.3610	8.3581
	0.6			10.8773	10.8602	10.8600	8.3824	8.3712	8.3698
		3		11.32871	11.3032	11.3020	9.5315	9.2321	8.9821
		5		12.32765	12.13263	12.1314	10.10621	9.9632	9.3214
			0.4	10.8352	10.6210	10.6131	8.2641	8.2530	8.2421
			0.6	10.81032	10.54210	10.5421	8.18348	8.14201	8.0312

Figures 2(a) and 2(b) are designed to deliberate the effect of M on $f(\eta)$ and $\Theta(\eta)$ profile. The effect of M on $f(\eta)$ is plotted in fig. 2(a). The Lorentz force was generated by the significant rise of M, acting against the flow pattern. As a result, the velocity of nano, hybrid, and trihybrid nanofluid cases declined rapidly. The temperature graph for the M factor is shown in fig. 2(b). According to the pictorial lay-out the $\Theta(\eta)$ field enhances as the strength of M improves. The predicted increase suggests that employing the hybrid nanofluid Ag-Al_2O_3-TiO_2/blood improves the resistive force.

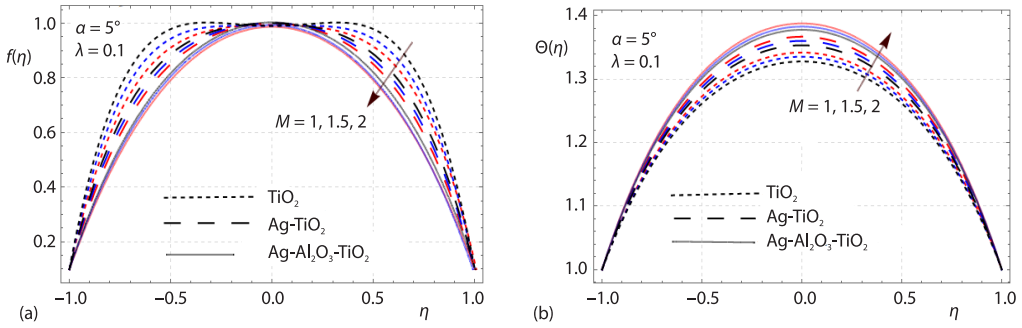

Figure 2. Influence of M on (a) $f(\eta)$ and (b) $\theta(\eta)$

The effect of α (angle) on $f(\eta)$ and $\Theta(\eta)$ are depicted pictorially in figs. 3(a) and 3(b) for nano, hybrid, and trihybrid nanofluid. As the degree of inclination increases, the trajectories of $f(\eta)$ show more substantial degradation, as shown in fig. 3(a). Furthermore, as seen in fig. 3(b), the progressive tendency of inclination (α) leads to an intensification in $\Theta(\eta)$. The temperature is more immediate when employing Ag-Al_2O_3-TiO_2/blood tri-hybrid nanofluids, as seen in both figures.

Figures 4(a) and 4(b) demonstrates the effect of E on $f(\eta)$ and $\Theta(\eta)$ fields utilizing three distinct types of nanofluids. The $f(\eta)$ and $\Theta(\eta)$ fields are increased with higher magnitude of E, as seen in the figs. 4(a) and 4(b). Obviously, the E field behaves as an accelerative strength, diminishing the resisting strength and as result boosting the $f(\eta)$ and $\Theta(\eta)$ gradually. Hence, we from pictorial representation that $f(\eta)$ and $\Theta(\eta)$ fields of Ag-Al_2O_3-TiO_2/blood shows greater behavior as compared to mono and hybrid nanofluid.

Figures 5(a) and 5(b) shows that the $f(\eta)$ and $\Theta(\eta)$ fields of three different types of nanofluids vary within divergent-convergent channels under the effect of ϕ_{TiO_2}, ϕ_{Ag}, $\phi_{Al_2O_3}$. Figure 5(a) also shows that the $f(\eta)$ profile of nanofluids drops as the magnitude of ϕ_{TiO_2}, ϕ_{Ag}, $\phi_{Al_2O_3}$ rises, whereas the $\Theta(\eta)$ field shows the reverse trend in fig. 5(b).

Table 1 illustrates a typical value of the materials research findings. Table 2 illustrates an assessment of present findings with existing literature [23, 25, 26], with the perfect consistency indicating that the problem has been validated. The C_f values for the different input adjustments were calculated numerically and are shown in tab. 3. The values of C_f were calculated over the face of the walls using the converging and diverging strategy. The C_f increased more in the tri-hybrid nanofluid than in the nanoand hybrid nanofluid. During the converging channel, C_f was found to be higher as equated to diverging channel. The numerical values of the Nusselt number for tri-hybrid, hybrid and nanofluids were obtained at different magnitudes of model factors by adopting the theory of divergence and convergence streams, as shown in tab. 4.

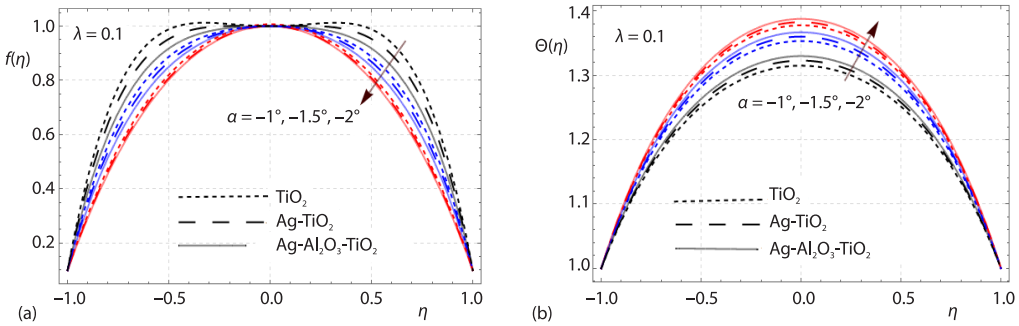

Figure 3. Influence of α on (a) $f(\eta)$ and (b) $\theta(\eta)$

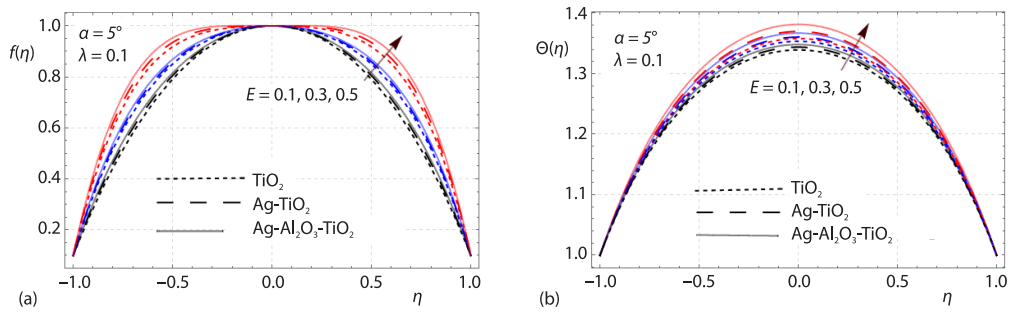

Figure 4. Influence of E on (a) $f(\eta)$ and (b) $\theta(\eta)$

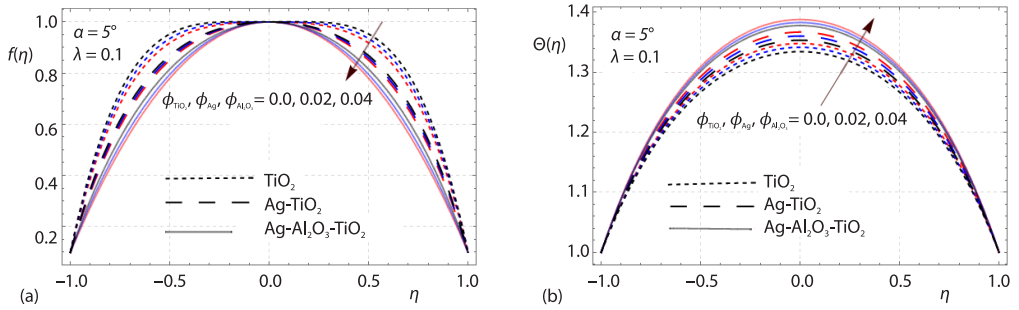

Figure 5. Influence of ϕ_{TiO_2}, ϕ_{Ag}, $\phi_{Al_2O_3}$, on (a) $f(\eta)$ and (b) $\theta(\eta)$

Conclusions

In this attempt, we scrutinize the mobility of a modified blood-based Casson hybrid nanofluid including three dissimilar nanomaterials in a convergent/divergent channel with stretchable/shrinkable walls. Computational investigations have indicated thatare as follows.

- The velocity of fluids has similar effect for factors M, α, E, and ϕ_{TiO_2}, ϕ_{Ag}, $\phi_{Al_2O_3}$, but opposite behavior for E.
- High magnitude of M, α, E, and ϕ_{TiO_2}, ϕ_{Ag}, $\phi_{Al_2O_3}$ enhanced the thermal profile.
- These patterns help us perceive the theoretical contribution of current problem subject to the medicinal area.
- The behavior of Nusselt numer and C_f for tri-hybrid nanofluid is more powerful when compared to those of nanoand hybrid nanofluids.

- The Ag, Al_2O_3, and TiO_2 nanomaterials play an essential part in evaluating the antimicrobial potency of *Escherichia coli* (bacteria that resides in human intestines normally) growth.
- With an increase in energy transmission, the values of electrical resistivity and pH enhanced. The objective of the design investigation would be use Ag, Al_2O_3 and TiO_2 nanomaterials for drug delivery.

Acknowledgment

The authors extend their appreciation to the Deanship of Scientific Research at Imam Mohammad Ibn Saud Islamic University for supporting this research work.

References

[1] Wagner, V., *et al.*, The Emerging Nanomedicine Landscape, *Nature Biotechnology*, *24* (2006), 10, pp. 1211-1217
[2] Jiang, Y., *et al.*, Dietary Copper Supplementation Reverses Hypertrophic Cardiomyopathy Induced by Chronic Pressure Overload in Mice, *The Journal of Experimental Medicine*, *204* (2007), 3, pp. 657-666
[3] Iftikhar, N., *et al.*, Inspection of Physiological Flow in the Presence of Nanoparticles with MHD and Slip Effects, *Journal of Thermal Analysis and Calorimetry*, *147* (2020), Nov., pp. 987-997
[4] Fullstone, G., *et al.*, Modelling the Transport of Nanoparticles under Blood Flow Using an Agent-Based Approach, *Scientific Reports*, *5* (2015), 1, pp. 1-13
[5] Li, Z., *et al.*, One-Pot Reaction Synthesize Biocompatible Magnetite Nanoparticles, *Advanced Materials*, *17* (2005), 8, pp. 1001-1005
[6] Ijaz, S., Nadeem, S., Biomedical Theoretical Investigation of Blood Mediated Nanoparticles (Ag-Al_2O_3/blood) Impact on Hemodynamics of Overlapped Stenotic Artery, *Journal of Molecular Liquids*, *248* (2017), Dec., pp. 809-821
[7] Dykman, L., Khlebtsov, N., Gold Nanoparticles in Biomedical Applications: Recent Advances and Perspectives, *Chemical Society Reviews*, *41* (2012), 6, pp. 2256-2282
[8] Riaz, A., *et al.*, Role of Hybrid Nanoparticles in Thermal Performance of Peristaltic flow of Eyring-Powell Fluid Model, *Journal of Thermal Analysis and Calorimetry*, *143* (2021), 2, pp. 1021-1035
[9] Shahzadi, I., Bilal, S., A Significant Role of Permeability on Blood Flow for Hybrid Nanofluid through Bifurcated Stenosed Artery: Drug Delivery Application, *Computer methods and programs in biomedicine*, *187* (2020), Apr., 105248
[10] Chamkha, A. J., *et al.*, Numerical Analysis of Unsteady Conjugate Natural-Convection of Hybrid Water-Based Nanofluid in a Semicircular Cavity, *Journal of Thermal Science and Engineering Applications*, *9* (2017), 4, pp. 1-15
[11] Waqas, H., *et al.*, Thermal Analysis of Magnetized Flow of AA7072-AA7075/BloodBased Hybrid Nanofluids in a Rotating Channel, *Alexandria Engineering Journal*, *61* (2022), 4, pp. 3059-3068
[12] Hussain, Z., *et al.*, Entropy Analysis in Mixed Convective Flow of Hybrid Nanofluid Subject to Melting Heat and Chemical Reactions, *Case Studies in Thermal Engineering*, *34* (2022), June, 101972
[13] Ramzan, M., *et al.*, Hydrodynamic and Heat Transfer Analysis of Dissimilar Shaped Nanoparticles-Based Hybrid Nanofluids in a Rotating Frame with Convective Boundary Condition, Scientific Reports, *12* (2022), 1, pp. 1-17
[14] Hassan, A., *et al.*, Heat Transport Investigation of Hybrid Nanofluid (Ag-CuO) Porous Medium Flow: Under Magnetic Field and Rosseland Radiation, *Ain Shams Engineering Journal*, *13* (2022), 5, pp. 1-13
[15] Mousavi, S. M., *et al.*, Numerical Study of Biomagnetic Fluid-Flow in a Duct with a Constriction Affected by a Magnetic Field, *Journal of Magnetism and Magnetic Materials*, *473* (2019), Mar., pp. 42-50
[16] Bhatti, M. M., *et al.*, Intra-Uterine Particle-Fluid Motion through a Compliant Asymmetric Tapered Channel with Heat Transfer, *Journal of Thermal Analysis and Calorimetry*, *144* (2021), 6, pp. 2259-2267
[17] Abdelsalam, S. I., *et al.*, Electro-Magnetically Modulated Self-Propulsion of Swimming Sperms Via Cervical Canal, *Biomechanics and Modelling in Mechanobiology*, *20* (2021), 3, pp. 861-878
[18] Bhaumik, B., *et al.*, Combined Impact of Brownian Motion and Thermophoresis on Manoparticle Distribution in Peristaltic Nanofluid-Flow in an Asymmetric Channel, *International Journal of Ambient Energy*, *43* (2021), 1, pp. 5064-5075
[19] Mekheimer, K. S., *et al.*, Biomedical Simulations of Nanoparticles Drug Delivery to Blood Hemodynamics in Diseased Organs: Synovitis Problem, *International Communications in Heat and Mass Transfer*, *130* (2022), Jan., 105756

[20] Sadeghy, K., *et al.*, Magnetohydrodynamic (MHD) Flows of Viscoelastic Fluids in Converging/Diverging Channels, *International Journal of Engineering Science*, *45* (2007), 11, pp. 923-938
[21] Jeffery, G. B., The 2-D Steady Motion of a Viscous Fluid, The London, *Edinburgh, and Dublin Philosophical Magazine and Journal of Science*, *29* (1915), 172, pp. 455-465
[22] Hamel, G., Spiralförmige Bewegungen zäher Flüssigkeiten, *Jahresbericht der deutschen mathematiker-vereinigung*, *25* (1917), pp. 34-60
[23] Dogonchi, A. S., Ganji, D. D., Investigation of MHD Nanofluid-Flow and Heat Transfer in a Stretching/Shrinking Convergent/Divergent Channel Considering Thermal Radiation, *Journal of Molecular Liquids*, *220* (2016), Aug., pp. 592-603
[24] Zheng, D., *et al.*, The Flow and Heat Transfer Characteristics in a Rectangular Channel with Convergent and Divergent Slit Ribs, *International Journal of Heat and Mass Transfer*, *141* (2019), Oct., pp. 464-475
[25] Ahmed, N., *et al.*, Thermal Radiation Effects on Flow of Jeffery Fluid in Converging and Diverging Stretchable Channels, *Neural Computing and Applications*, *30* (2018), 8, pp. 2371-2379
[26] Mishra, A., *et al.*, Roles of Nanoparticles and Heat Generation/Absorption on MHD Flow of Ag-H_2O Nanofluid Via Porous Stretching/Shrinking Convergent/Divergent Channel, *Journal of the Egyptian Mathematical Society*, *28* (2020), 1, pp. 1-18
[27] Kafoussias, N. G., Tzirtzilakis, E. E., Biomagnetic Fluid-Flow over a Stretching Sheet with Non-Linear Temperature Dependent Magnetization, *Zeitschrift für angewandte Mathematik und Physik ZAMP*, *54* (2003), 4, pp. 551-565

Paper submitted: January, 1 2022
Paper revised: March 21, 2022
Paper accepted: March 14, 2022